Songklanakarin J. Sci. Technol.
46 (1), 38–44, Jan. – Feb. 2024

http://www.sjst.psu.ac.th

Original Article

Immunohistochemical study of 3-mercaptopyruvate sulfurtransferase in the digestive system of the lesser bamboo rat (*Cannomys badius*) in relation to cyanide detoxification

Thanakul Wannaprasert[1*], Jettapol Likidkarnchanakornkij[1], and Depicha Jindatip[2]

[1] *Department of Biology, Faculty of Science, Chulalongkorn University, Pathum Wan, Bangkok, 10330 Thailand*

[2] *Department of Anatomy, Faculty of Medicine, Chulalongkorn University, Pathum Wan, Bangkok, 10330 Thailand*

Received: 8 December 2023; Revised: 16 January 2024; Accepted: 6 February 2024

Abstract

The lesser bamboo rat (*Cannomys badius*), a fossorial rodent distributed in Indochina, has the ability to feed on cyanogenic plants that normally induce cyanide poisoning and lead to cell death. Immunohistochemical staining was used for localizing 3-mercaptopyruvate sulfurtransferase (MST), a cyanide-detoxifying enzyme, in the digestive organs of *C. badius*. The results revealed MST-positive staining in gastric parietal cells, columnar epithelial cells in the large intestine, hepatocytes, and some endocrine cells in the pancreatic islets. Specifically, cecal and colonic epithelial cells and pericentral hepatocytes were relatively strongly stained. The present study suggests that MST in the parietal cells and the endocrine pancreas is not involved in cyanide detoxification but in the regulation of acid and hormone secretion. It is also postulated that cyanide produced by microbial fermentation of food in the cecum is primarily detoxified by MST in cecal epithelial cells and subsequently neutralized further by MST in the colon and liver. The digestive system of *C. badius* reflects a protective mechanism against cyanide toxicity allowing it to survive a diet of cyanogenic plants.

Keywords: epithelial distribution, gastrointestinal tract, immunohistochemistry, rodent

1. Introduction

The lesser bamboo rat (*Cannomys badius*) is a single species within its monotypic genus, which is sister to other bamboo rats *Rhizomys* within the same tribe (Rhizomyini). Skull and external morphologies that distinguish *C. badius* from other bamboo rats include a much smaller skull with a relatively longer rostrum and sagittal crest, smooth instead of granulated footpads, two instead of three abdominal pairs of teats, and a vertical white stripe of fur on the head (Lekagul & McNeely, 1988; Norris, 2017). *Cannomys badius* is found across Indochina where it has a fossorial lifestyle, excavating long complex tunnels in montane forests, cultivated plantations or even grassy areas. Its diet is comprised of plant roots and tubers growing within its burrows and also shoots and fallen fruits on the nearby ground. Additionally, evidence from some studies (Rurkkhum & Lauhachinda, 2008) and our observation from captive rearing have revealed that *C. badius* can feed on bamboo material and cassava, both of which have high cyanide contents (as cyanogenic glycosides).

Cyanide is a chemical compound that contains the cyano group (-C≡N). The most cytotoxic form of cyanide is hydrogen cyanide (HCN) in either gaseous or liquid condition (Reid, Jett, Platoff Jr, Yeung, & Babin, 2016). Cyanide blocks the electron transport chain in the mitochondria, and consequently ATP production is gradually depleted, leading to cell apoptosis (Lin *et al.*, 1998; Nagahara, Ito, & Minami, 1999). Cyanide is readily absorbed through the skin and mucous membranes lining the respiratory and gastrointestinal

*Corresponding author
Email address: thanakul@gmail.com

tracts. An acidic environment can facilitate a more rapid absorption (Narkowicz, Polkowska, & Namieśnik, 2013; Reid *et al.*, 2016). In mammals, particularly herbivores consuming cyanogenic plants (in forms of cyanogenic glycosides), the lethal effects of cyanide poisoning can be attenuated by two enzymes: rhodanese and 3-mercaptopyruvate sulfurtransferase (MST) (Nagahara *et al.*, 1999; Pedre & Dick, 2021). Reactions catalyzed by these two enzymes differ in their substrates and take place in different subcellular compartments. However, both yield the same detoxification product, converting cyanide into thiocyanate (SCN^-), a much less toxic molecule that is then excreted in the urine. Relatively little attention has previously been paid to MST, but interest in MST has increased sharply in recent years due to its roles related to key cellular processes.

While rhodanese activity is found only in mitochondria, MST activity is detected in both the cytosol and mitochondria across a wide range of organs with a cell type-specific activity within each organ. The highest MST levels are unanimously detected in the kidney and liver (Akahoshi *et al.*, 2020; Aminlari, Gilanpour, Taghavianpour, & Veseghi, 1989; Nagahara *et al.*, 1999; Tomita, Nagahara, & Ito, 2016). Low MST levels are detected throughout the gastrointestinal tract (GIT) in rats and mice (Nagahara, Ito, Kitamura, & Nishino, 1998; Tomita *et al.*, 2016). In contrast, a high MST activity is observed in the intestine of the cane rat that feeds extensively on plants rich in cyanogenic glycosides (Sanni, Ige, Olagunju, & Olukade, 2020). In ruminants, the surface epithelium of the fermentation chambers of the stomach exhibits a high MST activity, and this is linked to their diet as the epithelial layer of these stomach regions is the first site that is directly exposed to digested cyanogenic foodstuffs (Aminlari *et al.*, 1989). Likewise, MST protein expression is reported to depend on the tissues/cells' exposure to cyanide, where an increased exposure to cyanide stimulates elevated MST expression (Ma & Pritsos, 1997; Nagahara *et al.*, 1999). Tissues containing abundant MST can withstand cyanide exposure, thereby making species with these tissues less susceptible to cyanide poisoning (Aminlari *et al.*, 1989; Nagahara *et al.*, 1999).

As mentioned above, the distribution of MST along the GIT has been studied only in a few mammals, and not in *C. badius*. The tissue distribution of MST varies among mammalian species, while the level of MST expression shows a tissue-dependent manner, being partly constrained by dietary type. The present work aimed to study the distribution of MST in the GIT epithelium, liver and pancreas of *C. badius*. To facilitate understanding, general histology of the GIT epithelium, liver and pancreas was preliminarily described. These findings can contribute to a better understanding of the defensive role of digestive organs against cyanide toxicity.

2. Materials and Methods

All experimental protocols were approved by the Animal Care and Use Committee of the Faculty of Science, Chulalongkorn University (Protocol Review No. 2123018). Five adult *C. badius* (two males and three females; body mass = 471.20 ± 79.72 g) collected from Sukhothai and Nong Bua Lamphu provinces, Thailand, were examined (Figure 1). The rats were euthanized by an overdose of isoflurane inhalation from a vaporizer (apAlert RM, Australia). The euthanized rats

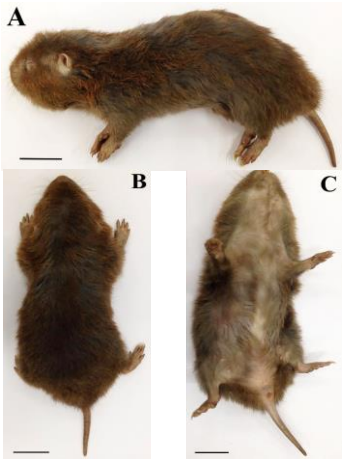

Figure 1. External morphology of *C. badius*. (A) Lateral view. (B) Dorsal view. (C) Ventral view. Scale bar = 3 cm.

were then perfused by 4% (w/v) paraformaldehyde in 0.05 M phosphate buffer solution pH 7.4 (PBS) via the left ventricle for 5 min, for fixation (BT100S, China). The tubular GIT, liver and pancreas were then dissected from the abdominal wall and washed gently with normal saline. The oral cavity, pharynx and gallbladder were not examined herein. The tubular GIT was divided into the esophagus, stomach, small intestine (duodenum, jejunum and ileum), cecum and colon (ascending, middle and descending parts). Tissues were immersed again in the same fixative (4% paraformaldehyde/PBS) overnight at 4 °C.

For histological examination, the fixed specimens were dehydrated in a graded series of ethanol from 70% to 100% (v/v) and embedded in paraffin. The paraffin blocks were cut into 4-μm-thick sections using a rotary microtome (Leica RM2255, England). The sections were stained with hematoxylin-eosin (H&E) to observe general tissue characteristics. Mounted slides were photographed under a compound light microscope (Leica DM750 LED, USA).

For MST detection by immunohistochemistry (IHC), tissues were rinsed with PBS and soaked sequentially in 20% and 30% (w/v) sucrose in PBS for two days. The tissues were then embedded and frozen in Tissue-Tek O.C.T. compound (Sakura Finetek, Japan), followed by cutting into 7-μm cryostat sections (Leica CM1950, USA). After treatment with 10% normal goat serum blocking solution (Vector Laboratories, USA) for 20 min, the sections were incubated overnight with rabbit anti-mouse MST antibody (MyBioSource, USA) at 4 °C. The optimal dilution of this primary antibody was 1:100. After washing three times with PBS for 5 min, the sections were incubated with anti-rabbit immunoglobulin G (MyBioSource, USA) at room temperature for 30 min, then with horseradish peroxidase-conjugated avidin for 30 min. For visualization of the immunoreaction, the sections were treated with diaminobenzidine-hydrogen peroxide solution and counterstained with hematoxylin. The sections incubated with just the antibody diluent lacking the primary antibody were internal negative controls. A case of mouse liver known to be positive for MST by IHC and Western blot analysis (Akahoshi *et al.*, 2020; Tomita *et al.*, 2016) was used as an external positive control. Positive IHC staining for MST imparted a brown color to the sections.

3. Results

The esophageal mucosa was covered by a keratinized stratified squamous epithelium without mucous-secreting cells (Figure 2A). The IHC analysis revealed that the esophageal epithelium was negatively stained for MST throughout its length (Figure 3A).

The stomach mucosa was divided into a non-glandular region at the fundus and a glandular region in the remaining parts, both of which were separated by the limiting ridge. The non-glandular region and the limiting ridge were lined by a keratinized stratified squamous epithelium, whereas the glandular stomach was lined by a simple columnar epithelium (Figure 2B-D). In the glandular region, the surface epithelium underwent invaginations to form gastric pits that led down to gastric glands where parietal cells and chief cells were located. The IHC analysis revealed that the keratinized non-glandular epithelium was negatively stained for MST, whereas the glandular portion showed positive staining for MST only in the parietal cells (Figure 3B).

In the small intestine, the mucosa had numerous finger-like projections of villi into the lumen. Branched and elongated villi could be observed in the duodenum and jejunum (Figure 2E). The epithelium of the villi was made up of simple columnar absorptive cells and a few goblet cells. The bases of villi were contiguous with intestinal glands (crypts of Lieberkühn). No positive staining for MST was observed along the small intestinal epithelium (Figure 3C).

The large intestinal mucosa lacked villi but still had intestinal crypts covered by a simple columnar epithelium with goblet cells. Unlike the numerous goblet cells in the colon, the cecum contained only a few goblet cells located on the lower part of the intestinal glands (Figure 2F). The colon exhibited noticeably numerous mucosal folds at its luminal surface. Each side of the fold in the ascending colon had intestinal glands at an unequal depth before becoming equal-depth glands in the middle and descending colon (Figure 2G-H). Throughout the length of the large intestine, numerous lymphoid aggregates were visible in the lamina propria beneath the epithelium. In the IHC analysis, columnar absorptive cells and some cells in cecal crypts, presumably enteroendocrine cells, reacted positively and strongly to MST staining (Figure 3D). In the colon, the absorptive cells were also positive, especially in the ascending colon. Cells in colonic crypts, including numerous goblet cells, did not show positive MST staining (Figure 3E). Noteworthily, the columnar cells of both the cecum and colon showed a stronger intracellular MST staining near the luminal surface than at the basal side of the epithelium (Figure 3D-E).

The liver was microscopically organized into an unclear boundary of hepatic lobules. Within each lobule, hepatocytes were arranged in one-cell-thick cords separated by sinusoids. Hepatocyte cords radiated outwards from the central vein to the periphery and anastomosed with one another, forming a labyrinthine structure (Figure 4A). Portal areas consisted of branches of the hepatic artery, portal vein and bile duct, all of which were wrapped in the connective tissue stroma. There was a positive MST staining in the hepatocytes, particularly in those cells around the central vein (Figure 4B).

As typically seen in other mammals, the pancreatic tissue consisted of both exocrine and endocrine cell types (Figure 4C). The exocrine portion was in the majority and its main component was serous acinar cells. Dispersed randomly within the exocrine tissue were light-staining cell clusters of islets of Langerhans. The MST-positive cells were scattered within the islets of Langerhans, but were absent in the exocrine tissue (Figure 4D).

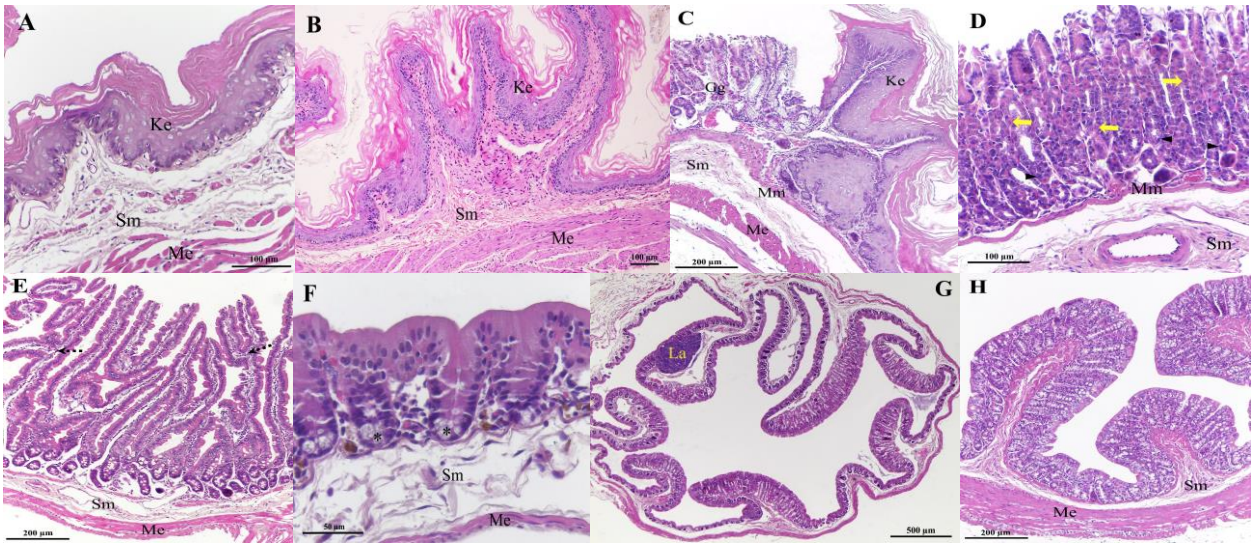

Figure 2. Photomicrographs of the epithelium of the GIT stained with H&E. Keratinized stratified squamous epithelium of the (A) esophagus, (B) non-glandular stomach and (C) limiting ridge. (D) Gastric glands of the glandular stomach containing mainly parietal cells (arrows) and chief cells (arrowheads). (E) Duodenal mucosa showing numerous elongated villi, the surfaces of which consisted of columnar epithelial cells and a few goblet cells. Branched villi (dashed arrows) were also noted. (F) Cecal epithelium containing columnar absorptive cells and a few goblet cells (asterisks) at the lower part of cecal crypts. (G) Ascending colon showing unequal-depth intestinal glands on each side of its mucosal fold. (H) Mucosal folds of the middle colon showing equal-depth intestinal glands. Gg, gastric glands; Ke, keratinized epithelium; La, lymphoid aggregates; Me, muscularis externa; Mm, muscularis mucosae; Sm, submucosa. Original magnification: ×200 for (A, B, D), ×100 for (C, E, H), ×400 for (F) and ×40 for (G)

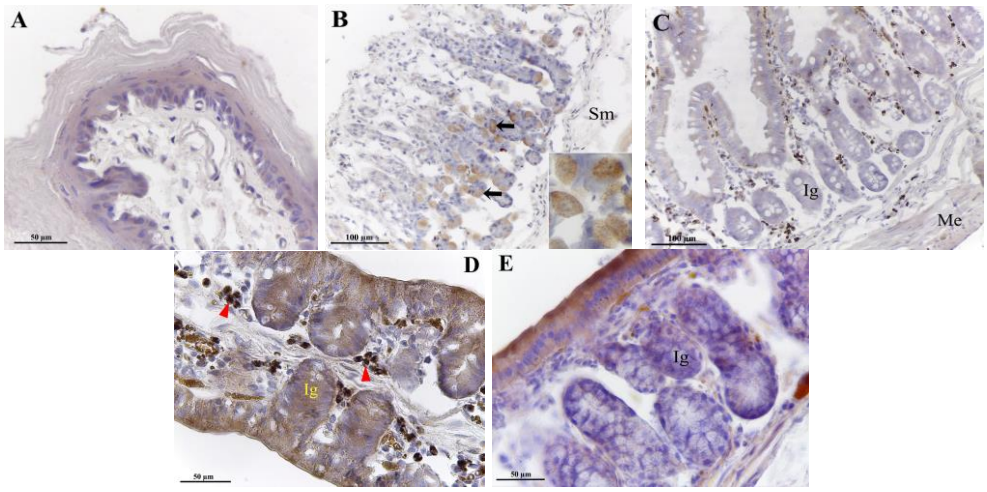

Figure 3. Photomicrographs of the epithelium of the GIT stained for MST by IHC. (A) Esophageal epithelium showing MST-negative staining. (B) Glandular stomach exhibiting MST-positive staining only in parietal cells (arrows). The inset shows some parietal cells at higher magnification. (C) Small intestinal epithelium without MST-positive staining. (D-E) Surface columnar cells of the cecum and ascending colon, respectively, showing intense intracellular MST staining near the luminal surface. Hemosiderin-laden macrophages (arrowheads in (D)) were indicated in the cecal lamina propria. Ig, intestinal glands; Me, muscularis externa; Sm, submucosa. Original magnification: ×400 for (A, D, E) and ×200 for (B, C)

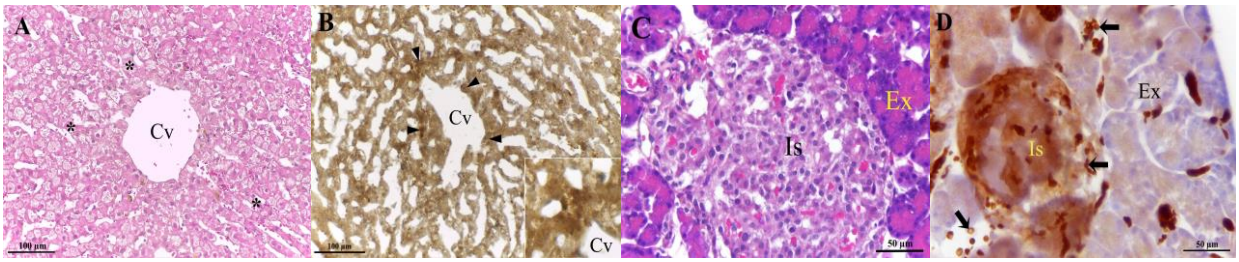

Figure 4. Photomicrographs of the liver and pancreas stained with H&E (A, C) and for MST by IHC (B, D). (A) Hepatic lobule displaying cords of hepatocytes (asterisks) radiating from the central vein toward the periphery of the lobule. (B) Hepatocytes showing MST-positive staining, particularly in the pericentral hepatocytes (arrowheads). A higher magnification of the pericentral hepatocytes is shown in the inset. (C) Pancreatic tissue consisting of the exocrine acini and endocrine cells within islets of Langerhans. (D) MST-positive cells found within islets of Langerhans. Erythrocytes (arrows) traveling through the pancreatic tissue were also positively stained. Cv, central vein; Ex, exocrine pancreas; Is, islets of Langerhans. Original magnification: ×200 for (A, B) and ×400 for (C, D)

All MST-positive cells observed in the GIT epithelium, liver and pancreas of *C. badius* are summarized in Table 1.

Table 1. A summary of MST-positive cells found in digestive organs of *C. badius*

Organs	MST-positive cells
Glandular stomach	Parietal cells
Cecum	Surface epithelial cells, some cells in cecal crypts
Colon	Surface epithelial cells
Liver	Hepatocytes
Pancreas	Some cells in islets of Langerhans

4. Discussion

Generally, the histological features of the gut epithelium, liver and pancreas of *C. badius* are similar to those of various other rodents. A meaningful feature was a unilocular-hemiglandular stomach, characterized by a single-chambered stomach with two distinct epithelia (Carleton, 1973). Also, complicated mucosal folds rich in goblet cells and lymphoid tissues in the large intestine were present, indicating their association with a fermentation process (Björnhag & Snipes, 1999; Walters *et al.*, 2014). In this section below, the distribution of MST and its roles in cyanide detoxification in the digestive organs are discussed.

No MST staining was found in the esophagus of *C. badius*. The absence of MST here may be due to the fact that the esophagus is mainly responsible for transporting food to the stomach in a short time, and no enzymatic digestion occurs here (Patricia & Dhamoon, 2022). In addition, thick keratinized layers can protect the esophageal epithelium from the permeation of toxic substances and so maintain the integrity of the epithelial cells (Meyer *et al.*, 2014).

In the stomach, MST was only detected in the parietal cells in the gastric glands. These cells secrete hydrochloric acid for acidification of the gastric lumen to create a barrier to the transit of pathogenic microbes, aid in protein digestion, and facilitate absorption of minerals.

Meanwhile, high acid levels can also potentially harm the gastric mucosa. Therefore, acid secretion by parietal cells requires rigorous control mechanisms via paracrine, endocrine and neural pathways (Engevik, Kaji, & Goldenring, 2020). In addition to cyanide detoxification, MST has a coactivity with cysteine aminotransferase in endogenous hydrogen sulfide (H_2S) synthesis (Magierowski, Magierowska, Kwiecien, & Brzozowski, 2015; Mard, Askari, Neisi, & Veisi, 2014). Exogenous H_2S is produced by gut commensal bacteria (Pedre & Dick, 2021). H_2S has been known to inhibit gastric acid secretion and protect the mucosal integrity against various damaging factors (Engevik *et al.*, 2020; Magierowski *et al.*, 2015). Since the stomach of *C. badius* is not the site for the microbial fermentation of ingested food that produces cyanide and H_2S, an important role of MST expression in parietal cells may be associated with the production of H_2S, acting via a paracrine pathway, to regulate acid secretion by the parietal cells and maintain gastric mucosal restoration.

The small intestine of *C. badius* lacked, or otherwise had little, MST expression. This result agrees with previous observations in rats and mice (Nagahara *et al.*, 1998; Tomita *et al.*, 2016). This implies that the small intestine of rodents is exposed to only low levels of cyanide, thereby reducing the necessity for a detoxification process. Degradation of cyanogenic glycosides by microbial enzymes, causing the release of cyanide, probably takes place to only a low level in the rodent small intestine.

In *C. badius*, the absorptive epithelial cells of the cecum and colon showed a relatively strong intracellular staining for MST near the intestinal luminal surface. Some MST-positive cells were found in the cecal crypts but there were none in the colonic crypts that consisted mostly of goblet cells. Thus, a strong polarization of MST expression is present in the large intestine, with the surface epithelium expressing MST strongly, and cells in the crypt showing a much lower or no MST expression. This differs from omnivorous rats and mice that show a weak staining in all of the intestines (Nagahara *et al.*, 1998; Tomita *et al.*, 2016). A trace level of MST may render the two species easily susceptible to cyanide toxicity. Based on a recent study, *C. badius* is considered to be a cecal fermenter (Likidkarnchanakornkij, Jindatip, & Wannaprasert, 2023). The cecum of *C. badius*, as in the ruminant stomach, is, therefore, the main habitat for fermenting microbes to take enzymatic action on cyanogenic foodstuffs and release cyanide into the lumen. A certain amount of cyanide may exit through the cecocolic orifice into the ascending colon. Thus, surface epithelial cells of the cecum and colon could be directly exposed to cyanide, explaining their strong MST expression for detoxification at their surfaces.

As unanimously seen in several previous studies (Akahoshi *et al.*, 2020; Aminlari *et al.*, 1989; Nagahara *et al.*, 1998; Tomita *et al.*, 2016), MST was expressed in the liver of *C. badius* and although distributed across the liver tissue, it was localized predominantly in hepatocytes around the central vein. This is concordant with earlier reports demonstrating the intense staining of pericentral hepatocytes in rats and mice (Nagahara *et al.*, 1998; Tomita *et al.*, 2016) and higher expression levels of detoxification-related genes in pericentral hepatocytes than in periportal hepatocytes (Cunningham & Porat-Shliom, 2021; Halpern *et al.*, 2017). Pericentral hepatocytes may act as the last defense of detoxifying toxic substances, e.g. cyanide, conveyed by hepatic sinusoids before draining into the central vein.

Tomita *et al.* (2016) reported high expression levels of MST in the endocrine pancreas of mice. This corresponds to the present study that showed MST-positive cells only in the pancreatic islets. Experiments in rats and rabbits revealed that chronic cyanide exposure via food intake does not exert any toxic effects on the pancreas (Mathangi, Deepa, Mohan, Govindarajan, & Namasivayam, 2000; Okolie & Osagie, 2000). Therefore, it seems that MST expression in the pancreas is not principally associated with cyanide detoxification. Instead, the role of MST in modulating the physiological roles of H_2S in pancreatic beta-cells is more likely. It has been proposed that H_2S inhibits insulin release and protects beta-cells against glucotoxicity-induced apoptosis (Okamoto *et al.*, 2013; Okamoto, Ishizaki, & Kimura, 2015). Possibly, the MST in the pancreas is involved in the synthesis of H_2S that is an essential part of the homeostatic mechanism for regulating hormone secretion and reducing cellular oxidative stress.

5. Conclusions

By IHC, MST was predominantly detected in the large intestine and liver of *C. badius*. That MST is abundant in the large intestine supports the idea that *C. badius* is a cecal fermenter. The results of this study allow us to postulate that the enzymatic digestion of ingested cyanogenic glycosides by commensal microbes liberates cyanide in the cecum and then continues into the colon. Cecal and colonic epithelial cells that are directly exposed to cyanide effectively detoxify it by MST activity in their cytoplasm and mitochondria. The remainder of the cyanide that is transported via the portal vein can then be neutralized by MST in the liver hepatocytes. These findings reflect a defensive adaptation of *C. badius*'s digestive system that allows it to withstand the toxic effects from cyanide and survive on cyanogenic food plants.

Acknowledgements

This project was funded by the 90th Anniversary of Chulalongkorn University Scholarship. The authors also thank Mrs. Wanida Buasorn for the help on methodologies.

References

Akahoshi, N., Minakawa, T., Miyashita, M., Sugiyama, U., Saito, C., Takemoto, R., . . . Ishii, I. (2020). Increased urinary 3-mercaptolactate excretion and enhanced passive systemic anaphylaxis in mice lacking mercaptopyruvate sulfurtransferase, a model of mercaptolactate-cysteine disulfiduria. *Inter national Journal of Molecular Sciences*, *21*, 818. doi:10.3390/ijms21030818

Aminlari, M., Gilanpour, H., Taghavianpour, H., & Veseghi, T. (1989). Comparative studies on the distribution of rhodanese and beta-mercaptopyruvate sulfur transferase in different organs of sheep (*Ovis aries*) and cattle (*Bos taurus*). *Comparative Biochemistry and Physiology. C, Comparative Pharmacology and Toxicology*, *92*, 259–262. doi:10.1016/0742-8413(89)90050-9

Björnhag, G., & Snipes, R. L. (1999). Colonic separation mechanism in lagomorph and rodent species - a comparison. *Zoosystematics and Evolution*, *75*, 275–281. doi:10.1002/mmnz.19990750208

Carleton, M. D. (1973). A survey of gross stomach morphology in new world Cricetinae (Rodentia, Muroidea), with comments on functional interpretations. *Museum of Zoology, University of Michigan*, *146*, 1–42.

Cunningham, R. P., & Porat-Shliom, N. (2021). Liver zonation–revisiting old questions with new technologies. *Frontiers in Physiology*, *12*, 732929. doi:10.3389/fphys.2021.732929

Engevik, A. C., Kaji, I., & Goldenring, J. R. (2020). The physiology of the gastric parietal cell. *Physiological Reviews*, *100*, 573–602. doi:10.1152/physrev.00016. 2019

Halpern, K. B., Shenhav, R., Matcovitch-Natan, O., Toth, B., Lemze, D., . . . Golan, M. (2017). Single-cell spatial reconstruction reveals global division of labour in the mammalian liver. *Nature*, *542*, 352–356. doi:10.1038/nature21065

Lin, J. H-C., Weigel, H., Cotrina, M. L., Liu, S., Bueno, E., Hansen, A. J., . . . Nedergaard, M. (1998). Gap-junction-mediated propagation and amplification of cell injury. *Nature Neuroscience*, *1*, 494–500. doi:10.1038/2210

Likidkarnchanakornkij, J., Jindatip, D., & Wannaprasert, T. (2023). Morphology of the digestive system of the lesser bamboo rat (*Cannomys badius*). *Anatomia Histologia Embryologia*, *52*, 944–955. doi:10. 1111/ahe.12954

Lekagul, B., & McNeely, J. A. (1988). *Mammals of Thailand* (2nd ed.). Bangkok, Thailand: Darnsutha Press.

Ma, J., & Pritsos, C. A. (1997). Tissue-specific bioenergetic effects and increased enzymatic activities following acute sublethal peroral exposure to cyanide in the mallard duck. *Toxicology and Applied Pharmacology*, *142*, 297–302. doi:10.1006/taap. 1996.8045

Magierowski, M., Magierowska, K., Kwiecien, S., & Brzozowski, T. (2015). Gaseous mediators nitric oxide and hydrogen sulfide in the mechanism of gastrointestinal integrity, protection and ulcer healing. *Molecules*, *20*, 9099–9123. doi:10.3390/ molecules20059099

Mard, S. A., Askari, H., Neisi, N., & Veisi, A. (2014). Antisecretory effect of hydrogen sulfide on gastric acid secretion and the involvement of nitric oxide. *BioMed Research International*, *2014*, 480921. doi:10.1155/2014/480921

Mathangi, D. C., Deepa, R., Mohan, V., Govindarajan, M., & Namasivayam, A. (2000). Long-term ingestion of cassava (tapioca) does not produce diabetes or pancreatitis in the rat model. *International Journal of Pancreatology*, *27*, 203–208. doi:10.1385/IJGC: 27:3:203

Meyer, W., Schoennagel, B., Kacza, J., Busche, R., Hornickel, I. N., Hewicker-Trautwein, M., & Schnapper, A. (2014). Keratinization of the esophageal epithelium of domesticated mammals. *Acta Histochemica*, *116*, 235–242. doi:10.1016/j.acthis.2013.07.008

Nagahara, N., Ito, T., Kitamura, H., & Nishino, T. (1998). Tissue and subcellular distribution of mercaptopyruvate sulfurtransferase in the rat: confocal laser fluorescence and immunoelectron microscopic studies combined with biochemical analysis. *Histochemistry and Cell Biology*, *110*, 243–250. doi:10.1007/s004180050286

Nagahara, N., Ito, T., & Minami, M. (1999). Mercaptopyruvate sulfurtransferase as a defense against cyanide toxication: molecular properties and mode of detoxification. *Histology and Histopathology*, *14*, 1277–1286.

Narkowicz, S., Polkowska, Ż., & Namieśnik, J. (2013). Determination of formaldehyde and cyanide ion in human nasal discharge by using simple spectro photometric methods. *Open Chemistry*, *11*, 16–24. doi:10.2478/s11532-012-0132-0

Norris, R. W. (2017). Family Spalacidae (muroid mole-rats). In D. E. Wilson, T. E. Jr Lacher, & R. A. Mittermeier (Eds.), *Handbook of the mammals of the world Vol. 7. Rodents II*. (pp. 108–142). Barcelona, Spain: Lynx Edicions.

Okamoto, M., Ishizaki, T., & Kimura, T. (2015). Protective effect of hydrogen sulfide on pancreatic beta-cells. *Nitric Oxide*, *46*, 32–36. doi:10.1016/j.niox.2014. 11.007

Okamoto, M., Yamaoka, M., Takei, M., Ando, T., Taniguchi, S., Ishii, I., et al. (2013). Endogenous hydrogen sulfide protects pancreatic beta-cells from a high-fat diet-induced glucotoxicity and prevents the development of type 2 diabetes. *Biochemical and Biophysical Research Communications*, *442*, 227–233. doi:10.1016/j.bbrc.2013.11.023

Okolie, N. P., & Osagie, A. U. (2000). Differential effects of chronic cyanide intoxication on heart, lung and pancreatic tissues. *Food and Chemical Toxicology*, *38*, 543–548. doi:10.1016/S0278-6915(00)00020-X

Patricia, J. J., & Dhamoon, A. S. (2022). *Physiology, Digestion* [StatPearls Version]. Retrieved from https://www.ncbi.nlm.nih.gov/books/NBK544242/

Pedre, B., & Dick, T. P. (2021). 3-Mercaptopyruvate sulfurtransferase: an enzyme at the crossroads of sulfane sulfur trafficking. *Biological Chemistry*, *402*, 223–237. doi:10.1515/hsz-2020-0249

Reid, F. M., Jett, D. A., Platoff Jr, G. E., Yeung, D. T., & Babin, M. (2016). *Animal models for testing antidotes against an oral cyanide challenge*. Maryland, MD: National Institutes of Health.

Rurkkhum, S., & Lauhachinda, V. (2008). Fossoring ecology and food habits of lesser bamboo rat (*Cannomys badius*). *Journal of Wildlife in Thailand*, *15*, 89–98.

Sanni, A. A., Ige, O. M., Olagunju, G. B., & Olukade, B. A. (2020). Partially purified 3-mercaptopyruvate sulphurtransferase obtained from the intestine of cane rat (*Thryonomys swinderianus*) as a detoxifier of cyanide. *Asian Journal of Biochemistry, Genetics and Molecular Biology*, *6*, 1–9. doi:10.9734/ AJBGMB/2020/v6i230146

Tomita, M., Nagahara, N., & Ito, T. (2016). Expression of 3-mercaptopyruvate sulfurtransferase in the mouse. *Molecules*, *21*, 1707. doi:10.3390/molecules21121 707

Walters, J., Marais, S., Johnson, O., Bennett, N. C., Alagaili, A. N., Mohammed, O. B., & Kotzé, S. H. (2014). The comparative gastrointestinal morphology of five species of muroid rodents found in Saudi Arabia. *Journal of Morphology*, *275*, 980–990. doi:10.1002/jmor.20270